

Study on magnetic separation device for scale removal from feed-water in thermal power plant

Saori Shibatani¹, Motohiro Nakanishi¹, Nobumi Mizuno¹, Fumihito Mishima¹, Yoko Akiyama¹,
Hidehiko Okada², Noriyuki Hirota²,
Hideki Matsuura³, Tatsumi Maeda³, Naoya Shigemoto³, Shigehiro Nishijima¹

Abstract— To improve the thermal power plant efficiency, we proposed a water treatment system with High Gradient Magnetic Separation (HGMS) system using superconducting magnet, which is applicable in high-temperature and high-pressure conditions. This is a method to remove the scale from feed-water utilizing magnetic force.

One of the issues for practical use of the system is how to extend continuous operation period. In this study, we succeeded in solving the problem by eliminating the deviation of captured scale quantity by each filter. In fact, in the HGMS experiment using the solenoidal superconducting magnet, it was shown that decrease in separation rate and increase in pressure loss were prevented, and the total quantity of captured scale increased by proper filter design.

The design method of the magnetic filter was proposed, and will be suitable for the long-term continuous scale removal in the feed-water system of the thermal power plant.

Index Terms— thermal power plant, scale, High Gradient Magnetic Separation (HGMS), solenoidal superconducting magnet

I. INTRODUCTION

In recent years, CO₂ emission is increasing associated with rapid the increase of world electricity demand. It is necessary to improve the efficiency of thermal power plants to realize low-carbon society, because they account for the most of CO₂ emission accompanied with the electric power generation. One of the factors declining thermal power generation efficiency is formation of scale by corrosion of pipework material in feed-water system [1]. The thermal conductivity of the scale is as low as 10% of pipework, so the scale adhesion decreases heat exchange efficiency. However, the effective methods for scale removal that can be applied to high temperature area of feed-water have not been developed

This research was partly supported by “Advanced Low Carbon Technology Research and Development Program (ALCA)” of Japan Science and Technology Agency (JST).

Saori Shibatani, Motohiro Nakanishi, Nobumi Mizuno, Fumihito Mishima, Yoko Akiyama, Shigehiro Nishijima are with Osaka University, A1 Bldg. 2-1 Yamadaoka, Suita, Osaka 565-0871, Japan (e-mail: shibatani@qb.see.eng.osaka-u.ac.jp).

Hidehiko Okada, Noriyuki Hirota are with National Institute for Materials Science, Tsukuba, Japan.

Hideki Matsuura, Tatsumi Maeda, Naoya Shigemoto are with Shikoku Research Institute Inc., Takamatsu, Japan.

though considerable quantity of scale is formed in high temperature area.

We proposed a high gradient magnetic separation (HGMS) system [2]-[3] using superconducting magnet as a new method of feed-water treatment. This is an effective method for scale removal from feed-water by magnetic force, because the main component of the scale is ferromagnetic magnetite (Fe₃O₄) in high temperature area of thermal power plant using All Volatile Treatment (AVT). We examined a continuous scale removal system under operation of thermal power plant by installing the HGMS device in high temperature area.

In our previous study, the separation rate of simulated scale achieved 98% under high-temperature and high-pressure condition (200 °C, 20 atm) simulating the thermal power plant [3]. One of the issues for practical use is that the scale is locally captured by filters near the inlet of separation unit. As a result, filters are easily blocked and separation efficiency decreases. In this study, we aimed to extend the continuous operation period with high separation rate by eliminating the deviation of scale capture quantity and preventing filter blockage. In this paper, we examined a filter design suitable for long-term scale removal by means of simulation and experiments.

II. METHODS

A. Particle trajectory simulation

Particle trajectories were calculated for examining the optimal magnetic separation conditions [4]-[5]. The target particle is magnetite which is the main component of the scale in high temperature area of thermal power plant using AVT. In the calculation, the magnetite particle diameter is set at 4 μm which is same as the experiment. At first, magnetic field and fluid around a magnetic wire were analyzed by finite element method (FEM) using ANSYS® Ver.10.0. Table I shows simulation conditions. Applied magnetic flux density is 2.0 T so that the magnetite and the magnetic filters are saturated magnetically considering the magnetic field distribution. Inlet fluid velocity is 0.6 m/s, which is a typical value of flow velocity in feed-water where we are planning to install the HGMS system. Magnetic force and drag force acting on the target particles were calculated by (1) and (2).

$$\mathbf{F}_D = 6\pi\eta r_p(\mathbf{v}_f - \mathbf{v}_p) \quad (1)$$

$$\mathbf{F}_M = \frac{4}{3} \pi r_p^3 (\mathbf{M} \cdot \nabla) \mathbf{H} \quad (2)$$

Magnetic force, \mathbf{F}_M and drag force, \mathbf{F}_D are described in 3 dimension. η is viscosity of the fluid, r_p is particle radius, \mathbf{v}_f is fluid velocity, \mathbf{v}_p is particle velocity, \mathbf{M} is magnetization of magnetite particle and \mathbf{H} is strength of magnetic field. Then particle trajectory was calculated by solving the motion equation of a magnetite particle shown in (3) with time evolution.

$$m\mathbf{a} = \mathbf{F}_M + \mathbf{F}_D \quad (3)$$

Fig.1 shows typical results of particle trajectory simulation. The area where magnetite is captured by a magnetic wire is defined as particle capture radius, r_p , when the initial position of magnetite particle was 3 mm upstream from the center of wire. The separation efficiency by each filter, α defined by (4) was calculated based on specific capture radius, r_a defined by (5) regarding the ratio of r_p and d_w where d_w is wire diameter.

$$\alpha [-] = r_a f \quad (4)$$

$$r_a [-] = \frac{r_p [mm]}{d_w [mm]} \quad (5)$$

f is filling factor of filters, indicating that α depends on wire diameter and mesh number of magnetic filter. Then magnetite capture quantity by N-th filter, Q_n was calculated from α and initial input of magnetite, Q_{input} shown in (6). The magnetite capture ratio by each filter was calculated from Q_n and total quantity of captured magnetite by all filters, Q_{Total} shown in (7).

$$Q_n [mg] = \left(Q_{input} [mg] - \sum_{k=1}^{n-1} Q_k [mg] \right) \times \alpha \quad (6)$$

$$\text{Capture ratio by each filter} [\%] = \frac{Q_n [mg]}{Q_{Total} [mg]} \times 100 \quad (7)$$

TABLE I
Simulation condition

Filter material	430 ss, galvanized iron
Wire diameter of filter	0.34 mm, 1.0 mm
Applied magnetic field: B_0	2.0 T
Fluid	water (293 K, $\eta=1.0 \times 10^{-3}$ Pa · s)
Inlet velocity of fluid: V_0	0.6 m/s

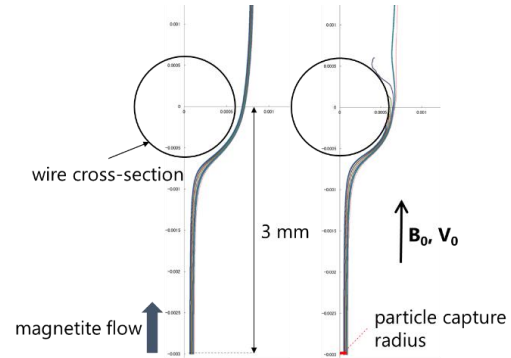


Fig. 1. Result of Fe_3O_4 particle trajectory simulation. (Magnetic field; left: 0 T, right: 2 T)

B. HGMS Experiment

HGMS experiment on magnetite (4.0 μm in average diameter, 0.4 T in saturated magnetization) was conducted to evaluate the performance of magnetic filters at room temperature. Table II shows specification of solenoidal superconducting magnet used for this experiment.

Fig.2 and Fig.3 show experimental setup and schematic diagram, respectively. Water in main piping is circulated by circulating pump (120 L/min in maximum). Magnetite suspension is injected to mainstream by injection pump (800 mL/min in maximum) and then mixed by static mixer. After that, mainstream is flown into the magnetic separation unit in solenoidal superconducting magnet. Fig.4 shows magnetic filters installed in separation unit. After the magnetic separation, the treated water is guided to the membrane filter (2 μm , 0.1 μm) and returns to the tank. The inner diameter of flow channel is 55 mm and the diameter of magnetic filter is 51 mm.

Table III shows filter conditions decided by the results of particle trajectories. In filter condition A, uniform mesh filters were used. In filter condition B, mesh opening becomes smaller as close to the outlet so as to equalize the quantity of captured magnetite. The total number of magnetic filters is 12 in both cases.

In Experiment 1, capture quantity of each filter was measured for two filter conditions. This experiment aimed to examine the difference between condition A and B in distribution of the captured magnetite. The concentration of magnetite was 270 ppb in the feed-water and the experiment was continued until the total injected magnetite became 40 mg. Iron concentration of dissolved particles captured by each filter was measured by inductively-coupled plasma atomic emission spectrometer (ICP-AES) (ICPS-7500, Simadzu Corp.) to calculate the capture ratio by each filter with (7).

In Experiment 2, temporal changes of separation rate and pressure loss of magnetic filters in addition to total quantity of captured magnetite were measured to verify the performance of magnetic filters designed in Experiment 1. The concentration of magnetite was observed to be 10 ppm when the blockage of magnetic filters was caused. The mainstream was sampled from sampling valves located at inlet and outlet of magnetic separation unit. Separation rate was calculated by (8) using iron concentration of the samples measured by ICP-

AES. The pressure gauges located at inlet and outlet of separation unit were also measured every 5 minutes.

$$\text{Separation rate [\%]} = \frac{C_{\text{Outlet}} [\text{ppm}]}{C_{\text{Inlet}} [\text{ppm}]} \times 100 \quad (8)$$

C_{Outlet} and C_{Inlet} are iron concentration of mainstream at outlet and inlet of separation unit, respectively.

Flow velocity is 0.6 m/s and applied magnetic flux density is 2.0 T in both in Experiment 1 and 2.

TABLE II

Specification of solenoidal superconducting magnet

Type	Cryogen-free superconducting magnet
Mode number	JMTD-10T100E3
Bore diameter	100 mm
Height	460 mm
Maximum magnetic flux density	10 T

TABLE III

Filter conditions

	Condition A	Condition B			
Wire diameter [mm]	0.34	1.0			
Mesh number	20	2	4	6	10
Mesh opening [mm]	0.93	11.7	5.35	3.23	1.54
α in eq.3 [-]	0.11	0.030	0.058	0.083	0.13

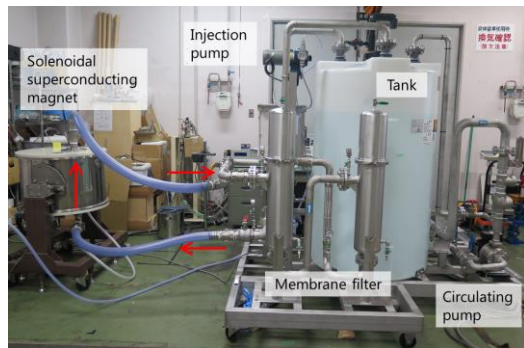


Fig. 2. Experimental setup.

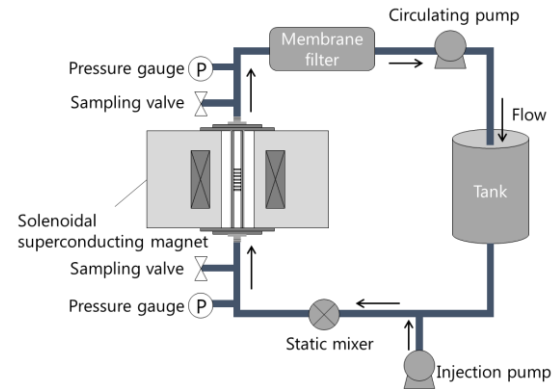


Fig. 3. Schematic diagram of experimental setup.



Fig. 4. Magnetic filter of separation unit. (Inlet side in filter condition B)

III. RESULTS AND DISCUSSION

Fig.5 and Fig.6 show the results of Experiment 1, with the calculated results by (4) to (7). Fig.5 shows magnetite capture rate by each filter in condition A. The filter material is stainless steel 430. In this case, magnetite was locally captured and the captured quantity decreased as closed to the outlet side. This result means upstream filters are easily blocked when the identical filters were used.

Fig.6 shows the result in condition B. The filter material is galvanized iron. The standard deviation of magnetite capture rate was 3.4 in condition B while 29 in condition A. So it was experimentally confirmed that the deviation of captured magnetite quantity by each filter was eliminated in condition B, in comparison with in condition A. In addition, it can be said that the results of simulation was properly performed because the calculated and experimental values indicated the similar tendency in both filter conditions. From these results, it is expected that filter blockage by captured magnetite is prevented in condition B which can extend the continuous operation period of HGMS system.

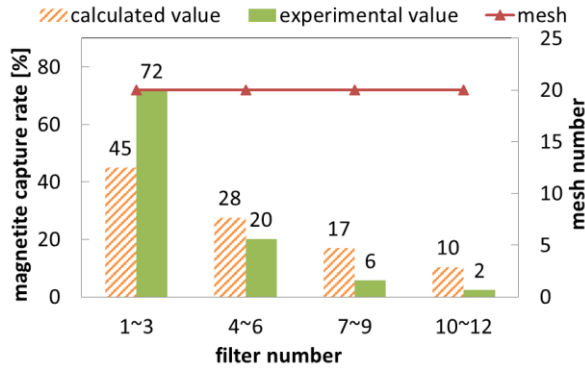


Fig. 5. Magnetite capture rate by each filter in filter condition A. (Slash bar graphs are calculated value, filled bar graphs are experimental value and line graph is mesh number.)

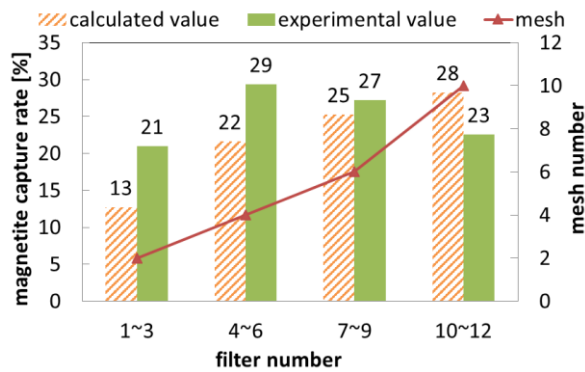


Fig. 6. Magnetite capture rate by each filter in filter condition B. (Slash bar graphs are calculated value, filled bar graphs are experimental value and line graph is mesh number.)

Fig.7 and Fig.8 show the results of Experiment 2. Fig.7 shows temporal changes of separation rate of magnetite and pressure loss of magnetic filter in condition A. The separation rate decreases with increase in pressure loss. The separation rate was 97% at the first 5 minutes. Meanwhile, the separation rate decreased after 10 minutes and it sharply dropped to 40% at 20 minutes though 78% at 15 minutes. On the other hand, the pressure loss gradually increased until 20 minutes, and became almost constant after 20 minutes. The final value of pressure loss was 13.5 kPa while initial value was 10.0 kPa.

Fig.8 shows temporal changes of separation rate and pressure loss in condition B. Decrease in separation rate and increase in pressure loss were prevented in comparison with Fig.7. The reason ought to be that the deviation of captured magnetite quantity by each filter was eliminated in condition B as expected in Experiment 1. The initial value of separation rate was 89% and it kept almost constant until 10 minutes. The minimum separation rate was 64%. On the other hand, the pressure loss slowly increased from 9.5 kPa to 10.5 kPa and it kept almost constant after 15 minutes.

In addition, the total quantity of magnetite captured by magnetic filter was 11.2 g in condition A and 16.3 g in condition B. So the total capture quantity of magnetite increases by proper magnetic filter design.

From these results, it can be said that we succeeded in the design of magnetic filter suitable for the long-term treatment

at room temperature. In addition, it is thought that the appropriate time to conduct backwashing of magnetic filter can be estimated by monitoring the pressure loss, for high-efficient scale removal.

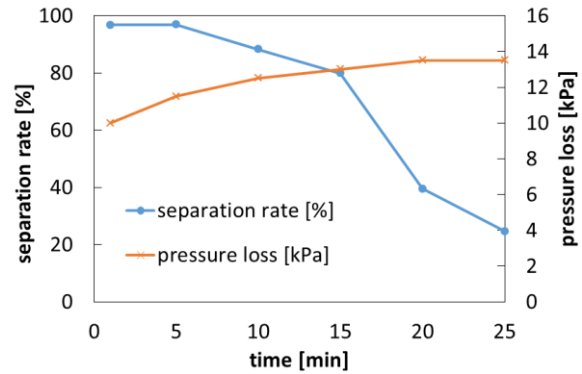


Fig. 7. Separation rate and pressure loss in filter condition A.

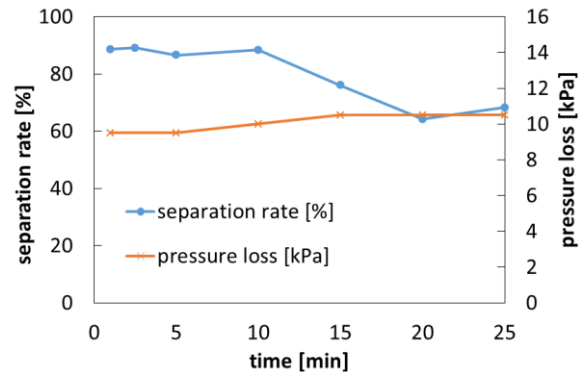


Fig. 8. Separation rate and pressure loss in filter condition B.

IV. CONCLUSION

Scale removal by HGMS was considered to improve thermal power plant efficiency. The magnetic filters were designed to eliminate the deviation of scale capture quantity by each filter to extend the continuous operation period. We succeeded in the design of the magnetic separation system suitable for long-term treatment by particle trajectory simulation and HGMS experiments. HGMS system should be ready for practical use for long-term scale removal from feed-water by means of the developed design method in this work. This technique will contribute to reduce CO₂ emissions originate in the electric power generation.

REFERENCE

- [1] X. Zhong, X. Wu, E. Han, "The characteristic of oxide scales on T91 tube after long-term service in an ultra-supercritical coal power plant," *J. of Supercritical Fluids*, vol. 72, 2012, pp. 68–77.
- [2] S. Nishijima, K. Takeda, K. Sato, T. Okada, S. Nakagawa, and M. Yoshiwa, "Applicability of superconducting magnet to high gradient magnetic separator," *IEEE Trans. Magn.*, vol. 14, no. 2, pp.573-576, 1987
- [3] N. Mizuno, F. Mishima, Y. Akiyama, H. Okada, N. Hirota, H. Matsuura, T. Maeda, N. Shigemoto, S. Nishijima "Removal of iron oxide with superconducting magnet high gradient magnetic separation from feed-water in thermal plant," *IEEE Trans. Appl. Supercond.*, Vol. 25, no. 3, 2015

- [4] H. Okada, K. Mtsuhashi, T. Ohara, E-R. Whitby, H. Wada
“Computational Fluid Dynamics Simulation of High Gradient Magnetic
Separation” *Separation Science and Technology*, 40: 1567-1584, 2005.
- [5] S. Hayashi, F. Mishima, Y. Akiyama, and S. Nishijima, “Development
of High Gradient Magnetic Separation System for a Highly Viscous
Fluid,” *IEEE Trans. Appl. Supercond.*, Vol. 20, no. 3, pp945-948, 2010